Journal of Civil Engineering and Architecture 19 (2025) 339-348
doi: 10.17265/1934-7359/2025.07.004

Investigation of Early Geopolymerization Process of Fly Ash-Based Geopolymer Paste Using Pattern Recognition

Lateef N. Assi
University of South Carolina, Dept. of Civil and Environ. Engineering, Columbia, SC 29208, USA

Abstract: Development of sustainable construction materials has been the focus of research efforts worldwide in recent years. Concrete is a major construction material; hence, finding alternatives to ordinary Portland cement is of extreme importance due to the high levels of carbon dioxide emissions associated with its manufacturing process. This study investigates the geopolymerization process. Specimens with, two different water/binder weight ratios, 0.30 and 0.35, were monitored using acoustic emission. Results show that there is a significant difference in the acquisition data between the two different water/binder weight ratios. In addition, acoustic emission can be used to beneficially monitor and investigate the early geopolymerization process. The acoustic emission data were processed through pattern recognition. Two clusters were identified, assigned to a specific mechanism depending on their characteristics. SEM observations were coincided with pattern recognition findings.

Keywords: Geopolymer concrete, compressive strength, silica fume activating solution, geopolymerization process, acoustic emission.

1. Introduction

Due to the global concern about CO_2 emissions, it is well accepted that a new kind of cement is in needed to replace Portland cement with improved environmental, mechanical, and durability performance. Portland cement is responsible for 7% of total CO_2 emission [1], and it has been stated that every ton of Portland cement releases roughly one ton of CO_2 emissions [2] due to the high energy required for production. Alkali activated geopolymer cement is one potential alternative to Portland cement. It may help to address the mentioned drawbacks once the mechanical and chemical behaviors are understood.

Alkali activated cement (geopolymer cement) is an inorganic polymer, produced by reacting a source of aluminate silicate, such as fly ash, slag, or metakaolin, with an activating solution. Either the common activating solution: sodium silicate, sodium hydroxide and water; or the alternative activating solution: sodium hydroxide, silica fume and water may be used. Several researchers [3-8] have shown that alkali activated concrete has enhanced mechanical properties. For instance, this material demonstrates high early and final compressive strength, low sulfate attack, resistance against acid erosion, and better performance under high temperatures when compared with conventional Portland cement concrete. However, the geopolymerization process is still ambiguous and needs to be identified to better understand, and then enhance, the chemical, microstructural, and mechanical properties.

Acoustic emission has been used to monitor chemical phenomena in both materials due to its high sensitivity. More specifically, acoustic emission has been utilized to monitor the early hydration process of different types of cement such as calcium aluminate in paste samples [9-11]. Results of acoustic emission have been characterized, and assigned to hydration

Corresponding author: Lateef N. Assi, assistant professor, research field: sustainable concrete; civil engineering materials; reinforced concrete.

mechanisms and compared to results gained by x-ray tomography. In addition, acoustic emission data was compared to the measured temperature of cement paste samples [12]. The early hydration of Portland cement has been assessed [13-15], and the acoustic emission technique was proven sensitive enough to monitor chemical and synthetic processes, as well as microcrack initiation.

Geopolymerization is a reaction producing silico-aluminates. Any source of pozzolanic materials, such as fly ash or slag, has high aluminate and silica portion and when dissolved in an alkaline solution, will lend itself to geopolymerization [16]. Several researchers have attempted to explain the geopolymerization process and its related mechanisms. Fernandez-Jimenez and Palomo investigated several factors including the amount of reactive silica, particle size distribution, and the vitreous phase content [17]. It was found that silica played a dominant role in the chemical reaction and that the aluminosilicate gel is the mainly responsible for mechanical properties [18]. Jaarsveld and Deventer explained the mechanism of geopolymerization according to Purdon; by liberation of silica, alumina and lime in presence of an activating solution, and then formation of aluminate-silicate hydrate. Generally, the geopolymerization mechanism can be summarized into dissolution of aluminate and silicate oxides due to hydroxide ions, orientation of dissolved products, and finally condensation and hardening [16]. Condensed products have poorly ordered structures (amorphous structure) due to the rapidness of the reaction [18]. However, most researches have not assigned the mechanism stages in regard to the time and temperature throughout the geopolymerization process. Understanding the time of mechanism occurrence, and how the geopolymerization process happens, will help to better understand and further the development of geopolymer concrete.

In this study, two fly ash-based geopolymer pastes with water/binder weight ratios 0.3 and 0.35 were monitored. The activating solution used was a mixture of silica fume, sodium hydroxide, and water. Acoustic emission sensors were used to monitor the early geopolymerization process for 80 hours with an AEwin data acquisition system. The data was post-processed with AEwin and NOESIS to cluster the acoustic emission data. Two clusters were identified and assigned to specific mechanisms including dissolution (bubbles occurring in this stage), and hardening (micocracks occurring in this stage).

2. Methods and Materials

Two different water/binder to weight ratios were chosen, 0.30 and 0.35 respectively. The reason for choosing these water/binder ratios is because with a lower water/binder weight ratio (lower than 0.3), the initial time setting is rapid (less than three minutes), however, for a higher water/binder weight ratio of 0.35, initial setting did not occur during the test period.

The materials used for fabrication of the fly ash-based geopolymer paste included fly ash (ASTM class F) and activating solution (sodium hydroxide mixed with silica fume and distilled water). The fly ash was sourced from Wateree Station in South Carolina. Chemical compositions of the fly ash source are shown in Table 1. The activating solution material sources were silica fume (Sikacrete 950DP, densified powder silica fume), sodium hydroxide (97-98 purity, DudaDiesel), and water. The mixture proportions of the fly ash-based geopolymer paste are provided in Table 2.

2.1 Activating Solution:

The silica fume based activating solution was a mixture of sodium hydroxide flakes dissolved in water, and silica fume powder. Following the addition of silica fume powder the mixture was stirred for two minutes. The mixing of silica fume with sodium hydroxide and water resulted in an exothermic process (exceeds 80 ºC [176 ºF]). The activating solution was kept in a closed container in an oven at 75 ºC (167 ºF) for approximately 12 hours to assure that the sodium hydroxide flakes and silica fume powder were completely dissolved. The

Table 1 XRF chemical analysis of fly ash.

Chemical analysis	Wateree Station wt.%
Silicon Dioxide	53.5
Aluminum Oxide	28.8
Iron Oxide	7.47
Silicon Dioxide and Aluminum Oxide	89.8
Calcium Oxide	1.55
Magnesium Oxide	0.81
Sulfur Trioxide	0.14
Loss on Ignition	3.11
Moisture Content	0.09
Total Chlorides	-------
Available Alkalies as NaO_2	0.77

Table 2 Mixture proportions.

Fly ash-based geopolymer paste (water/binder*)	Fly ash, kg/m^3 (lb/ft^3)	Water, kg/m^3 (lb/ft^3)	w/b* ratio	Sodium hydroxide, kg/m^3 (lb/ft^3)	Silica fume, kg/m^3 (lb/ft^3)
Mix 1: silica fume based activating solution paste (0.30)	474 (29.6)	175 (10.9)	0.30	61.6 (3.81)	46.2 (2.92)
Mix 2: silica fume based activating solution paste (0.35)	474 (29.6)	204 (12.7)	0.35	61.6 (3.81)	46.2 (2.92)

*Binder (b) = combined weight of the fly ash, sodium hydroxide, and silica fume.

water/binder ratio was calculated by dividing the water weight by the summation of dried fly ash sodium hydroxide and silica fume weight. The activating solution was mixed with the fly ash for three minutes manually and then each water/ binder ratio was cast in four 3.8 cm X 3.8 cm X 11.4 cm (1.5 in X1.5 in X4.5 in) plastic molds. The plastic molds were vibrated for ten seconds, thermocouples were inserted inside the samples, and the acoustic emission sensors were attached. The mixing procedure described above is the same as described in Assi et al; 2016 [7].

2.2 Experimental Test Setup:

ADiSP16-channel acoustic emission system was used in this investigation. WDI-automated sensors, broadband acoustic emission sensors, (40 dB integral preamplifier) 200-900 kHz frequency range, were used to monitor and collect acoustic emission data [19].

A background noise test was conducted in the material laboratory at the University of South Carolina to identify the threshold prior to initiating the actual test, and the threshold was set to 31 dB. During the hydration test, all of the specimens were kept inside a plastic chamber with the ambient temperature of 22 ± 3°C. To isolate the specimens from outside vibrations, a low-density foam pad was placed on the floor of the plastic chamber [20]. Nine broadband sensors were used in each test; eight attached on the sides of the specimens. Four geopolymer paste molds for each water/binder ratio were used. One sensor was attached on a plastic sheet as a control sensor to monitor potential noise. The test setup is shown in Figure 1. Vacuum grease was used as a couplant between the plastic molds and sensors. Temperature and humidity data loggers were used to monitor the humidity and temperature inside the plastic chamber. Each test was conducted for a period of 80 hours.

3.1 Results and Discussions

Geopolymerization is referred to a chemical reaction that involves occurring silico-aluminates [16]. It takes place when an activating solution such as a mixture of silica fume, sodium hydroxide and water, are mixed with an aluminate-silicate source such as fly ash. The geopolymerization process can be summarized by a)

dissolution, with formation of mobile precursors through action of hydroxide ions, b) partial orientation of mobile precursors and c) precipitation where the mixturehardens into an inorganic polymeric structure. External heat and alkali content play strong roles in the geopolymerization process [21-26]. For instance, if external heat and pH concentration increase, the geopolymerization process will become rapid in comparison with the hydration process of conventional cement.

Due to rapid reactions, the structure of the geopolymerization products is amorphous. The main chemical products are composed of silicon and aluminum. The three-dimensional structure of amorphous product consists of poly (sialate) type (Si-O-Al-O-), the poly (sialate-siloxo) type (Si-O-Al-O-Si-O-), and the poly(sialate-disiloxo) type (Si-O-Al-O-Si-O-Si-O-) [27]. The geopolymerization process can be summarized as follows:

$$n(Si_2O_5, Al_2O_2) + 2nSiO_2 + 4nH_2O \xrightarrow{NaOH,KOH} n(OH)_3 - Si - O - \underset{|}{\overset{(-)}{Al}} - O - Si - (OH)_3$$

$$n(OH)_3 - Si - O - \underset{|}{\overset{(-)}{Al}} - O - Si - (OH)_3 \xrightarrow{NaOH,KOH} (Na,K)^{(+)} - \left(-Si(=O) - O - \underset{|}{\overset{(-)}{Al}}(=O) - O - Si(=O) - O - \right) + 4nH_2O \quad [27]$$

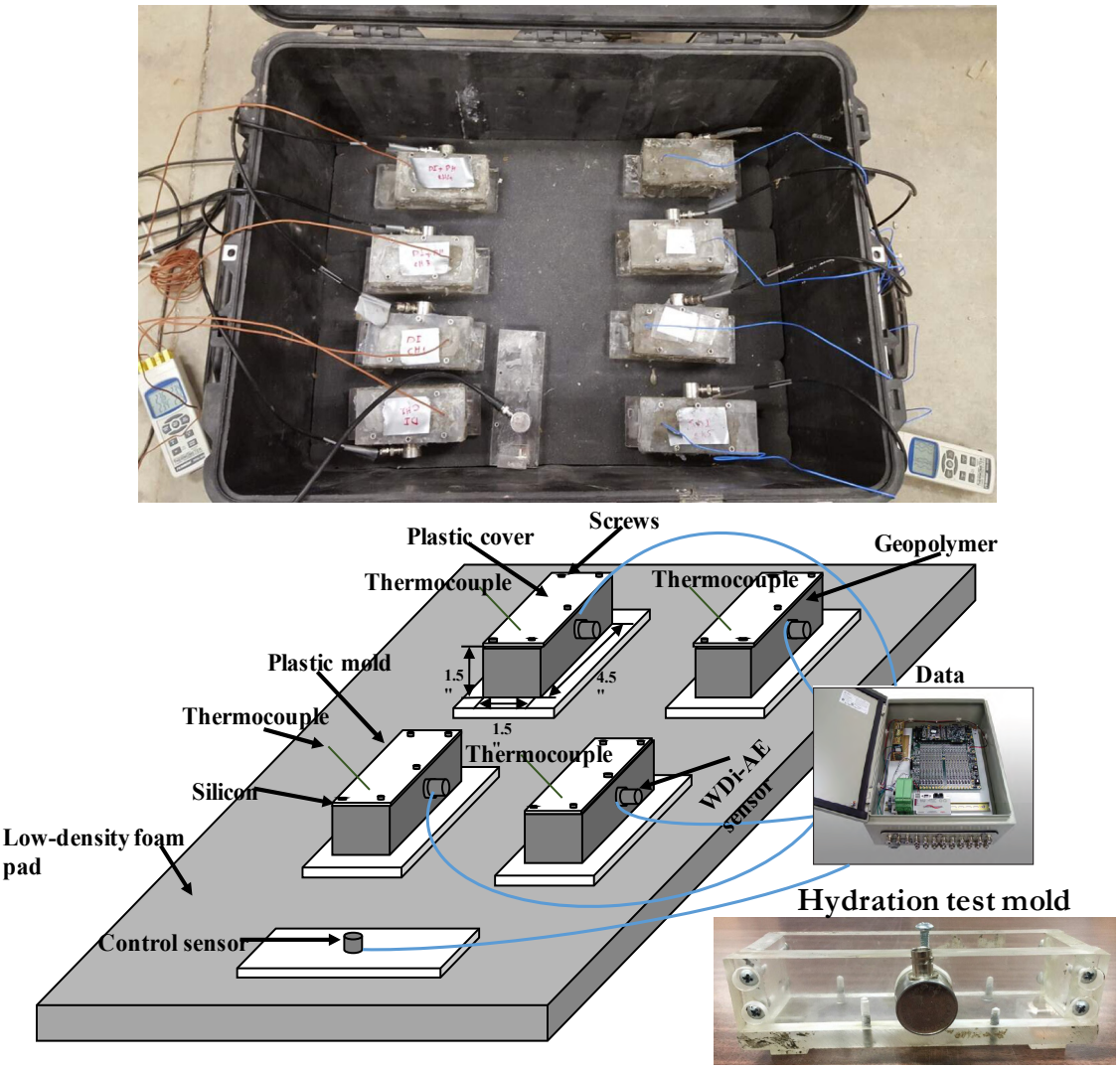

Fig. 1 Experimental test setup, scheme, and photograph of the real test.

3.2 Relationship between Acoustic Emission hits and Temperature History

The maximum internal temperatures were 34.5 ºC and 26.0 ºC for fly ash–based geopolymerization as shown in Fig. 2. The maximum temperature was observed at 0.28 and 0.45 hours after starting the tests, for water/binder weight ratios of 0.30 and 0.35, respectively. Furthermore, the temperature increase in the average accelerated rate region, which is the ascent part, was 9.40 ºC and 4.90 ºC for samples with water/binder weight ratios of 0.30 and 0.35. These observations show that fly ash-based geopolymer paste with lower water/binder weight ratio, geopolymerizes (reacts) faster and releases more heat compared to specimens with larger water/binder weight ratio. By comparing the maximum internal temperature for a conventional Portland cement paste to fly ash-based geopolymer paste, the heat of hydration tends to be higher than geopolymerization.

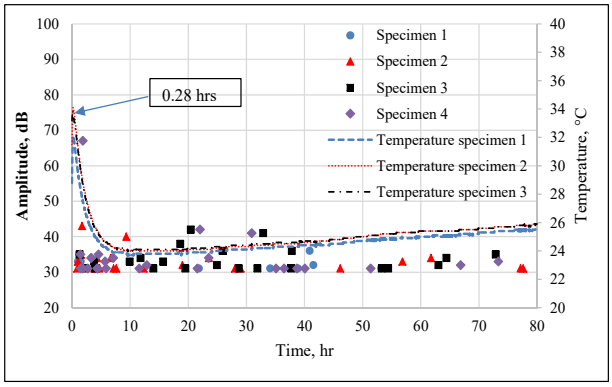

Water/binder ratio = 30%

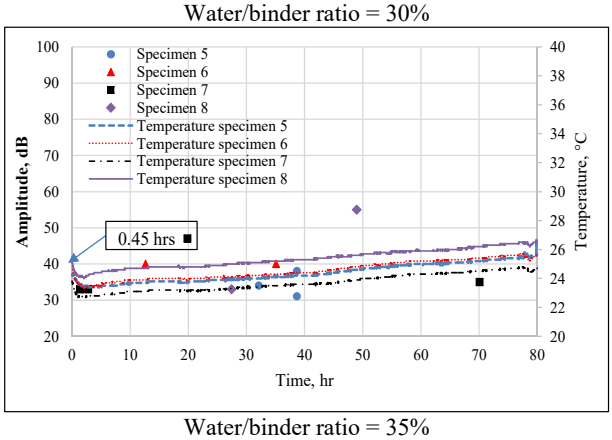

Water/binder ratio = 35%

Fig. 2 Amplitude of acoustic emission signals and temperature distribution during geopolymerization process.

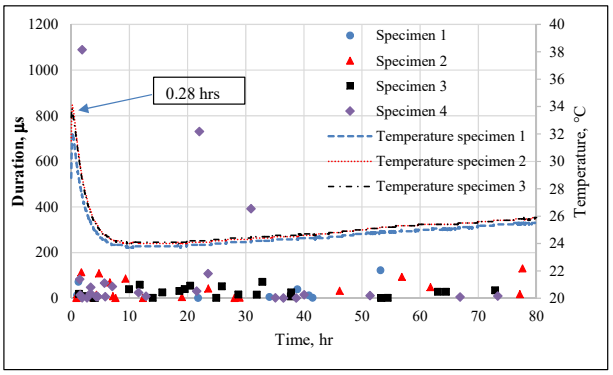

Water/binder ratio= 30%

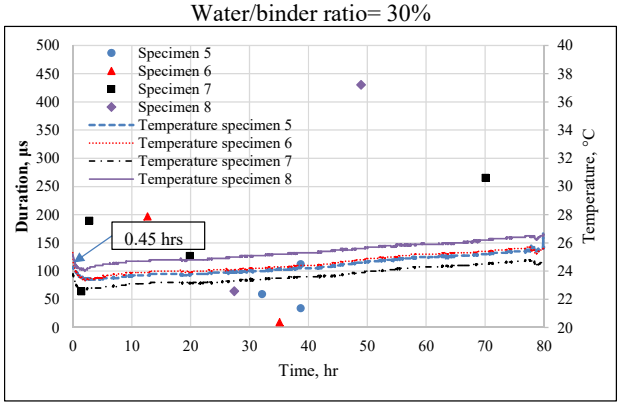

Water/binder ratio=35%

Fig. 3 Signal duration and temperature distribution during geopolymerization process.

This may be considered an advantage for fly ash-based geopolymer paste because lower internal heat may reduce microcrack initiation. Fig. 2 shows that a higher concentration of hits is precent when the temperature arrives to the peak with varied amplitudes for 0.30 water/binder ratio. However; hits are distributed throughout the test for 0.35 water/binder ratio. The difference in the number of hits is attributed to the increase in water content resulting in more available water to absorb the stress wave. The extra water may delay the geopolymerization process as well.

Fig. 3 show duration for 0.30 and 0.35 water/binder ratio, respectively. The average duration of both water/binder ratios is approximately the same.

As shown in Fig. 2 and 3, the acoustic emission signals near the maximum temperature have high amplitude and duration, and the rest of the test has a random distribution. Acoustic emission hits were observed early, and continue throughout the test. This phenomenon suggests a correlation between acoustic

emission hits and the geopolymerization process.

Fig. 4 shows cumulative signal strength for the two water/binder ratios. The cumulative signal strength for 0.30 ratio is higher than for the 0.35 water/binder ratio due to a higher number of acoustic emission hits. The extra water in the case of 0.35 water/binder ratio will absorb some of the energies, and the hardened phase occurred later, resulting in fewer potential microcracks. As shown in Fig. 4, the increase in CSS rate begins to occur after the acceleration region, and extends a few hours for both water/binder weight ratio. The first signal of the 0.30 and 0.35 water/binder weight ratio samples was recorded in the early stage of the geopolymerization process at 0.10 hours after test onset.

3.2 Scanning Electron Microscope Observations

Two geopolymer paste samples were prepared for Scanning electron microscope (SEM) observations. The geopolymer paste samples were taken from the mix that used for the main geopolymerization test. The SEM test was conducted at the University of South Carolina. The sample age was 14 days. In the Fig.5, the 0.35 and 0.30 paste samples are on the left and right of the figure respectively. Two different magnifications, 1000 and 6000, were conducted to identify the microstructure, reacted and unreacted particles. Image 5A shows many unreacted fly ash particles, while in the image 5B, it shows fewer unreacted fly ash particles. In addition, image 5C and 5D have a higher resolution, which shows the activating solution including sodium hydroxide surrounding fly ash particles. These images show that the geopolymerization process has begun already, and some of the fly ash particles have not dissolved due to lack of external heat. Image 5D shows the presences of microcracks, which will be confirmed in the upcoming section. The SEM images showed that the geopolymerization process has been started, and geopolymerization products are present as well as microcrack initiation.

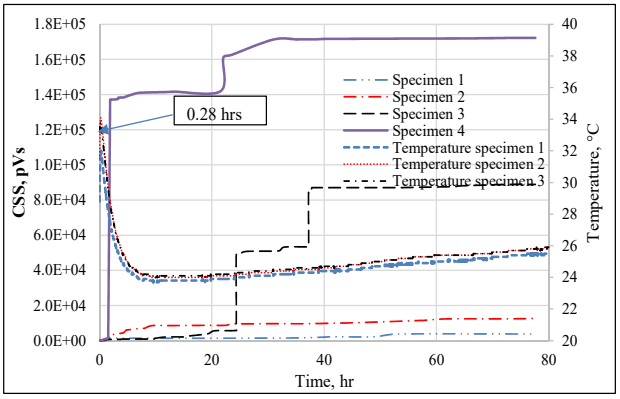

Water/binder weight ratio = 30%

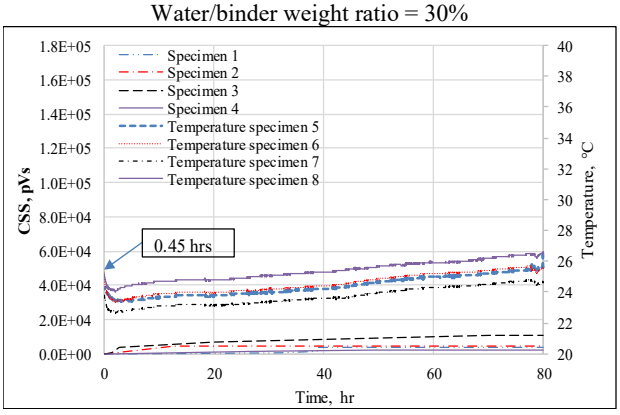

Water/binder weight ratio = 35%

Fig. 4 Cumulative Signal strength and temperature distribution during geopolymerization process.

3.3 Classification of Acoustic Emission Data and Assignment of Geopolymerization Mechanisms

To investigate different geopolymerization stages and mechanisms, the acoustic emission signals were processed using NOESIS software [21]. Unsupervised pattern recognition was chosen due to lack of background information related to acoustic emission data from the geopolymerization process. The features for clustering purposes were selected based on a feature correlation hierarchy diagram, which graphically illustrates correlations between features of the signals [21]. Features were normalized in the range of -1 to 1. Principle component analysis (PCA) was utilized for reducing the dimension of the data.

The algorithm for unsupervised clustering was k-means [21]. The k-means method is an iterative algorithm, which starts from assigning the data to initial randomized centers, and it is stopped when the resulted clusters are no longer changed [21].

Fig. 6a presents the unsupervised pattern recognition results for the water/binder ratio of 0.30. The attributed

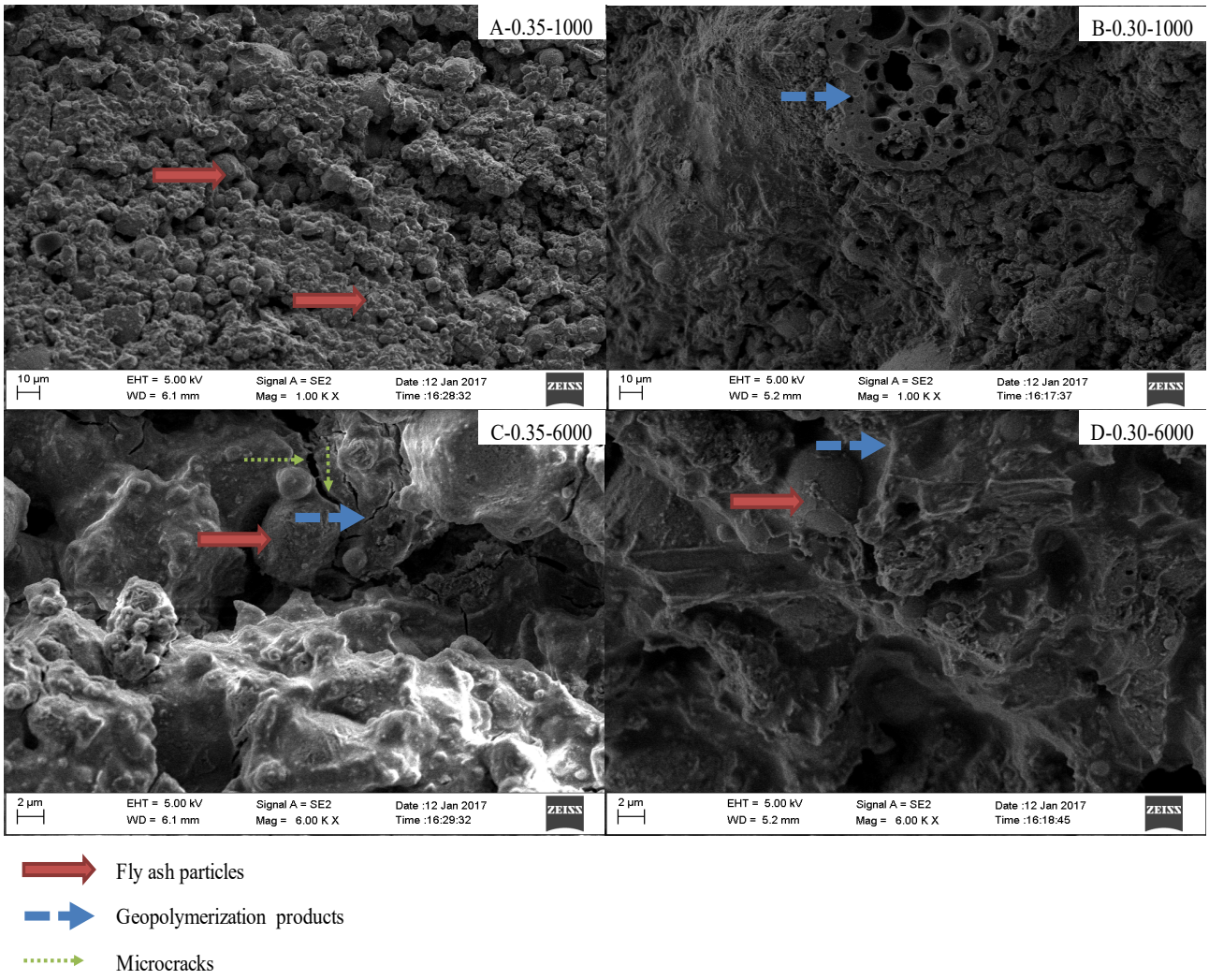

Fig. 5 SEM observation.

reason is that the potential mechanisms may occur at approximate the same time. This is different from what has been observed in Portland cement paste samples [9-11]. This can be interpreted as a gradual process of polymerization and simultaneous occurrence of the mechanisms.

The mechanism for cluster A can be dissolution of Si and Al atoms from the source material through action of hydroxide ions and consumption of water, fly ash, activating solution, and bubble formation. It is assumed that dissolution and consumption of material requires lower energy [10]. Moreover, dissolution and consumption are expected to be repetitive during the reaction because polarization is a gradual reaction and it takes time for the process to be completed. Hence it can be expected that the material such as water and fly ash are dissolving and reacting with the activating solution. They need to be dissolved initially and consumed to produce the final geopolymerization product; particularly, in the absence external heat, which enhances the geopolymerization process. These processes need less energy compared with formation of final products and microcracking. Dissolution and consumption produce signals with lower signal strength and amplitude.

Cluster B may be assigned to microcracks, chemical shrinkage, formation of the final geopolymerization products and setting or polycondensation/

polymerization of monomers into polymeric structures. The signals of cluster B have larger signal strength and amplitude, corresponding to large sources of energy. Formation of final products is expected to release most of the energy of the reaction. In addition, microcracking is always assumed to have high energy sources of the signals in acoustic emission [10]. Therefore, these signals can be assigned to mechanisms with higher sources of energy.

Fig. 6b presents unsupervised pattern recognition results for water/binder weight ratio of 0.35. Similar to the previous sample, in these specimens, there is no clear separation between two assigned clusters regarding the time of the experiment. The samples with water/binder weight ratio of 0.35 have data until 70 hours and no signals after that were observed. This may represent microcracks or shrinkage in these samples are reduced or delayed because of excessive water during reaction, and the geopolymerization process was slow, and incomplete as shown in the SEM section.

Cluster A` may be assigned to microcracks, chemical shrinkage, formation of final geopolymerization products and setting or polycondensation/polymerization of monomers into polymeric structures. The signals for this cluster have larger signal strength and amplitude, which shows a large source of energy. Formation of final geopolymerization products is the main part of the reaction, which is expected to release most of the energy of the reaction. In addition, microcracks are assumed to correspond to high energy sources of the signals [10]. Therefore, these signals may be assigned to mechanisms with higher sources of energy.

Cluster B` can be attributed to the dissolution of Si and Al atoms from the material source through action of hydroxide ions and consumption of water, fly ash and activating solution, and formation of bubbles. Signal strength and amplitude of the signals are less than for cluster A`.

As shown Fig. 6b, dissolution and consumption of material appear faster at the beginning of test, but they seem to have low-energy after 70 hours.

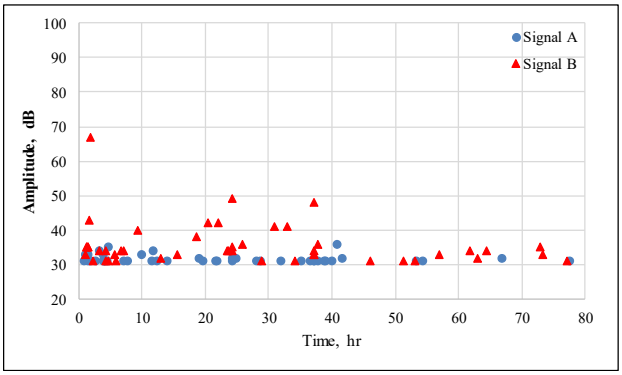

Water/binder weight ratio = 30%

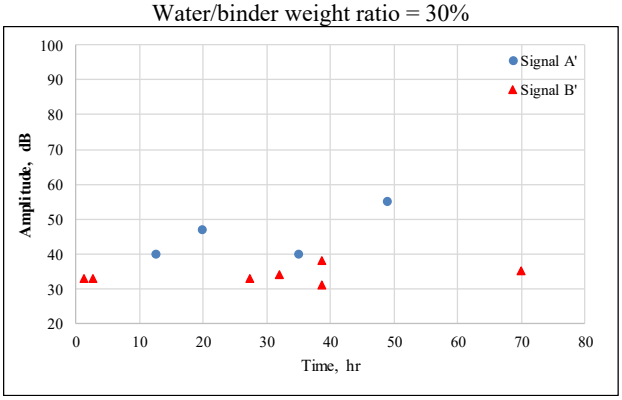

Water/binder weight ratio = 0.35%

Fig. 6 Principal component analysis for fly ash-based geopolymer paste.

The observation from these two clusters as shown in Fig. 6a, depict that most of the polymerization reaction happens in the first 70 hours in the case of 30% water/binder weight ratio. The reason is due to presence of the water and activating solution, which enhances the geopolymerization process. On the other hand, the acoustic emission data are fewer because the extra water delayed the initial time setting, and the produced stress wave should be strong enough to emit from a source.

The acoustic emission data clusters shown in Fig.6 (a, and b for 0.3 and 0.35 respectively) were assigned to the forming bubbles and microcrack initiations as well as slow geopolymerization reaction activity. Principle component analyses (PCA) shows there are two clusters assigned to the geopolymerization process mechanisms, as described earlier, and the two clusters occurred simultaneously.PCA analysis aided to understanding the geopolymerization process from the time of occurrence and standpoint of the mechanism initiation.

4. Conclusions

Acoustic emission was employed to investigate the fly ash-based geopolymerization process and to investigate the relationship between recorded signals and activities and mechanisms associated with fly ash-based geopolymer paste geopolymerization. Results of this study are summarized as follows:

Duration, signal amplitude, and signal strength of received signals had a correlation with hydration temperature distribution during fly ash-based paste geopolymerization.

The measured temperature readings indicate the geopolymerization process may have potential advantages in comparison with conventional cement.

Acoustic emission activity was correlated to the speed of the geopolymerization process.

Two clusters were identified for both water/binder ratios, and they occurred throughout the test.

The principal component analyses showed that most of the geopolymerization mechanisms occur at roughly the same time due to rapidness of geopolymerization process, unlike the hydration process of Portland cement.

The SEM observations were shown the geopolymerization process has been initiated at early time; however, several fly ash particles have not reacted yet in both of water/binder ratios samples.

Acknowledgments

This research is partially supported by the U.S. Department of Energy Office of Science, Office of Basic Energy Sciences, and Office of Biological and Environmental Research under Award Number DE-SC-00012530.

References

[1] Chen, C., Habert, G., Bouzidi, Y., Jullien, A., (2010). "Environmental impact of cement production: detail of the different processes and cement plant variability evaluation." Journal of Cleaner Production, 18(5), pp.478–485.

[2] Hasanbeigi, A., Menke, C. & Price, L., (2010). "The CO2 abatement cost curve for the Thailand cement industry." Journal of Cleaner Production, 18(15), pp.1509–1518.

[3] Wallah, S.E., (2000). "Drying Shrinkage of Heat-Cured Fly Ash-Based Geopolymer Concrete." CCSE journal, 3(12), pp.14–21.

[4] Hardjito, D., Wallah, S. E., Sumajouw, D. M J., Rangan, B. V., (2004). "On the development of fly ash-based geopolymer concrete." ACI Materials Journal, 101(6), pp.467–472.

[5] Sumajouw, D.M.J. et al., (2007). "Fly ash-based geopolymer concrete: Study of slender reinforced columns." Journal of Materials Science, 42(9), pp.3124–3130.

[6] Wallah, S.E., (2011). "Creep Behaviour of Fly Ash-Based Geopolymer Concrete." Civil Engineering, 12(2), pp.73–78.

[7] Assi, L.N., Deaver, E., ElBatanouny, M. K., Ziehl, P., (2016). "Investigation of early compressive strength of fly ash-based geopolymer concrete." Construction and Building Materials, 112, pp.807–815.

[8] Lloyd, N.A. & Rangan, B. V., (2010). "Geopolymer Concrete with Fly Ash." Second International Conference on Sustainable Construction Materials and Technologies, (January).

[9] Chotard, T., Rotureau, D. & Smith, A., (2005). "Analysis of acoustic emission signature during a luminous cement setting to characterize the mechanical behavior of the hard material." Journal of the European Ceramic Society, 25(16), pp.3523–3531.

[10] Chotard, T.J., Smith, A., Rotureau, D., et al., (2003). "Acoustic emission characterization of calcium aluminate cement hydration at an early stage." Journal of the European Ceramic Society, 23(3), pp.387–398.

[11] Chotard, T.J., Smith, A., Boncoeur, M.P., Fargeot, D., Gault, C., (2003)." Characterization of early stage calcium aluminate cement hydration by combination of non-destructive techniques: Acoustic emission and X-ray tomography." Journal of the European Ceramic Society, 23(13), pp.2211–2223.

[12] Pazdera, L., Topolar, L., Korenska, M., Smutny, J., Bilek, V., (2014.) "Advanced Analysis of Acoustic Emission Parameters during the Concrete Hardening for Long Time." 11th European Conference on Non-Destructive Testing, (Ecndt).

[13] Sayers, C.M. and Dahlin, A., (1993). "Propagation of ultrasound through hydrating cement pastes at early times." Advanced Cement Based Materials, 1(1), pp.12-21.

[14] Y. Lu, J. Zhang, Z. Li, Study on hydration process of early-age concrete using embedded active acoustic and non-contact complex resistivity methods, Constr. Build. Mater. 46 (2013) 183–192.

[15] Van Den Abeele, K. Desadeleer, W., De Schutter, G., Wevers, M., (2009). "Active and passive monitoring of the early hydration process in concrete using linear and

nonlinear acoustics." Cement and Concrete Research, 39(5), pp.426–432.

[16] Khale, D. & Chaudhary, R., (2007). "Mechanism of geopolymerization and factors influencing its development: A review." Journal of Materials Science, 42(3), pp.729–746.

[17] Fernández-Jiménez, A. &Palomo, A., (2003). "Characterization of fly ashes. Potential reactivity as alkaline cements." Fuel, 82(18), pp.2259–2265.

[18] Palomo, A., Grutzeck, M.W. & Blanco, M.T., (1999). "Alkali-activated fly ashes: A cement for the future." Cement and Concrete Research, 29(8), pp.1323–1329.

[19] Acoustic emission win version E4.30, Mist. Gro. Inc., Prin. Jun., NJ, 2004.

[20] Lura, P., Couch, O., Jensen, J., O., M., Weiss, J., (2009). "Early-age acoustic emission measurements in hydrating cement paste: Evidence for cavitation during solidification due to self-desiccation." Cement and Concrete Research, 39(10), pp.861–867.

[21] Al Bakri, A.M.M., Kamarudin, H., Bnhussain, M., Nizar, I. K., Rafiza, A. R., Izzat, A. M., (2011). "Chemical Reactions in the Geopolymerisation Process Using Fly Ash-Based Geopolymer: A Review." Journal of Applied Sciences Research, 7(7), pp.1199–1203.

[22] Duxson, P., Fernández-Jiménez, A., Provis, J. L., Lukey, G. C., Palomo, A., Van Deventer, J. S J, (2007). "Geopolymer technology: The current state of the art." Journal of Materials Science, 42(9), pp.2917–2933.

[23] Duxson, P., Provis, J. L., Lukey, G. C., Van Deventer, J. S J., (2007). "The role of inorganic polymer technology in the development of "green concrete." Cement and Concrete Research, 37(12), pp.1590–1597.

[24] Van Jaarsveld, J.G.S. & van Deventer, J.S.J., (2004). "The potential use of geopolymeric materials to immobilize toxic metals: Part I. theory and application." Minerals Engineering, 10(7), pp.201–251[22].

[25] Pacheco-Torgal, F., Castro-Gomes, J. &Jalali, S., (2008). "Alkali-activated binders: A review. Part 1. Historical background, terminology, reaction mechanisms and hydration products." Construction and Building Materials, 22(7), pp.1305–1314 [23].

[26] Silva, P. De, Sagoe-Crenstil, K. & Sirivivatnanon, V., (2007). "Kinetics of geopolymerization: Role of Al2O3 and SiO2." Cement and Concrete Research, 37(4), pp.512–518 [24].

[27] Davidovits, J., (1994). "Properties of Geopolymer Cements." First International Conference on Alkaline Cements and Concretes, pp.131–149.